ACTIVITY DEPENDENT STIMULATION INCREASES SYNAPTIC EFFICACY IN SPARED PATHWAYS IN AN ANESTHETIZED RAT MODEL OF SPINAL CORD CONTUSION INJURY

Jordan A. Borrell, Ph.D.[1,2], Dora Krizsan-Agbas, Ph.D.[3], Randolph J. Nudo, Ph.D.[2,4],

and Shawn B. Frost, Ph.D.[2,4]

Bioengineering Program[1], University of Kansas, Lawrence, KS, USA

Landon Center on Aging[2], University of Kansas Medical Center, Kansas City, KS, USA

Molecular & Integrative Physiology[3], University of Kansas Medical Center, Kansas City, KS, USA

Department of Rehabilitation Medicine[4], University of Kansas Medical Center, Kansas City, KS, USA

Figure Count: 8

Table Count: 3

Word Count (Abstract): 383

Word Count (Introduction): 1,033

Word Count (Discussion): 2,761

Corresponding Author: Shawn B. Frost, PhD, Dept. Rehabilitation Medicine, University of Kansas Medical Center.

Mail Stop: 1059, 3901 Rainbow Blvd., Kansas City, KS 66160, 913-588-5695, sfrost@kumc.edu.

Abstract

Objective. The purpose of this study was to assess the ability of intraspinal microstimulation, triggered by action potentials (spikes) recorded in motor cortex, to alter synaptic efficacy in descending motor pathways in an anesthetized rat model of spinal cord injury. *Approach.* Experiments were carried out in adult, male, Sprague Dawley rats with a moderate contusion injury at T8. Four weeks after SCI, and under ketamine/xylazine anesthesia, fine wire electromyographic (EMG) electrodes were implanted into four muscles of the right hindlimb. After exposure of the left motor cortex hindlimb area and laminectomy of the T13-L1 vertebrae, intracortical microstimulation (ICMS) and intraspinal microstimulation (ISMS) were used to determine the location of evoked hip movements in cortex and spinal cord, respectively. For activity-dependent stimulation sessions, a single shank, 16-channel, recording microelectrode was used to detect neuronal spikes in motor cortex that triggered ISMS in the spinal cord grey matter. Spinal cord injured rats were randomly assigned to one of four experimental groups differing by: a) cortical spike-ISMS stimulus delay (10 or 25 ms) and b) number of ISMS pulses (1 or 3). Activity-dependent stimulation sessions were conducted in three consecutive 1-hour conditioning bouts for a total of 3 hours. At the end of each conditioning bout, changes in synaptic efficacy were assessed using ICMS to examine the number of spikes evoked in spinal cord neurons during five minute test bouts. Evoked spikes were recorded, sorted, and displayed in post-stimulus spike histograms in 1-ms bins. Post-stimulus spike histograms and EMG recordings were characterized using stimulus triggered averaging techniques. *Main results.* The results showed that activity-dependent stimulation resulted in an increase in cortically-evoked spikes in spinal cord neurons at specific combinations of spike-ISMS delays and numbers of pulses. Efficacy in descending motor pathways was increased throughout all dorsoventral depths of the hindlimb spinal cord, including the ventral horn, in the vicinity of motor neurons. Changes were evident in some conditions as early as 1 hour after conditioning. EMG responses were never evoked with ICMS pre-or post-conditioning. *Significance.* These results show that

after a spinal cord contusion injury, activity-dependent stimulation, consisting of cortical spike-driven ISMS, can increase synaptic efficacy in spared pathways between motor cortex and spinal cord. This suggests that activity-dependent stimulation may serve as an effective therapeutic approach for enhancing descending motor control after spinal cord injury.

Introduction

Closed-loop neuromodulation systems have received increased attention in recent years as potential therapeutic approaches for treating neurological injury and disease. One type of closed-loop, activity dependent stimulation (ADS) paradigm utilizes extracellularly-recorded action potentials in one location to deliver small amounts of electrical current to another population of neurons. By artificially driving the temporal coupling of two synaptically connected populations of neurons, a change in the strength of synapses may occur between them. This phenomenon is based on the theories of Donald Hebb who described the process of synaptic plasticity between two hypothetical neurons: When presynaptic cell A reliably contributes to spiking of postsynaptic cell B, the functional strength of the synapse from A to B increases (Hebb, 1949). It is also believed that there is a congruent weakening of ineffective synapses (Stent, 1973). Currently, it is recognized that associative synaptic strengthening and weakening are implemented at synapses by long-term potentiation (LTP) and depression (LTD), respectively. The direction of synaptic change is strongly associated with the temporal coupling between presynaptic spiking and postsynaptic depolarization, with LTP occurring when pre- and postsynaptic activity occur together, and LTD occurring when pre- and postsynaptic activity do not occur together (Lisman, 1989). In addition, *in vitro* studies have noted an effect due to spike order, with LTP occurring when presynaptic inputs occurred first or were synchronous with postsynaptic spikes, and LTD occurring when presynaptic input followed postsynaptic spikes (Levy and Steward, 1983; Debanne et al., 1994, 1997; Fung et al., 2016). Commonly known as precise timing- and order-dependent plasticity, it has been shown that the sign and magnitude of LTP and LTD depend on the order and timing of pre- and postsynaptic spikes on the 10 ms time scale and that a 10-50 ms time delay increased spiking probability (Gerstner et al., 1996; Markram et al., 1997; Bi and Poo, 1999).

In an *in vitro* model of monosynaptically connected neurons, the effect of a stimulus initiated 10 ms before or after the onset of an excitatory postsynaptic potential (EPSP) showed that the EPSP

amplitude could be down- or up-regulated, respectively, depending on the precise timing of synapse activation (Markram et al., 1997). Later *in vitro* studies found that repetitive postsynaptic spiking within a time window of 20 ms after presynaptic activation resulted in LTP, whereas postsynaptic spiking within a window of 20 ms before the repetitive presynaptic activation led to LTD (Bi and Poo, 1998). These findings suggest that single synapses are modified according to the temporal relations of the electrical activity of the neurons in a network. Replication of the natural timing of pre- and post-synaptic events has been shown to potentiate, or condition, neuronal connections *in vivo* (Jackson et al., 2006), resulting in functional plasticity of motor cortex outputs.

To determine its potential clinical utility, ADS, an experimental paradigm based on the timing of pre- and post-synaptic events, is beginning to be tested in injury models. In a rat model of traumatic brain injury, it was shown that ADS can enhance synaptic efficacy between neurons in premotor and somatosensory cortex and result in rapid behavioral recovery in a skilled reaching task (Guggenmos et al., 2013). Importantly, the enhanced synaptic efficacy persists following the cessation of ADS conditioning. Other studies have provided support for the therapeutic potential of ADS after spinal cord injury. In a rat model of cervical spinal cord injury, it was shown that intraspinal microstimulation (ISMS), triggered by volitional muscle activity in the impaired forelimb, can improve behavioral performance in a forelimb reach and grasp task (McPherson et al., 2015). In non-human primates with a unilateral spinal cord transection, it was shown that epidural spinal cord stimulation triggered by neuronal spikes from the hindlimb motor cortex can restore weight-bearing locomotion of the paralyzed leg (Capogrosso et al., 2016).

Because SCI frequently occurs in the thoracic and lumbar cord, hindlimb motor function often is profoundly affected. ADS could potentially be used to enhance synaptic efficacy of descending pathways after such injuries. The purpose of the present study was to determine whether different spike-stimulus delays and number of ISMS pulses differentially increases synaptic efficacy in descending motor

pathways using an ADS paradigm in an anesthetized rat model of lower thoracic spinal cord contusion injury. Spike-timing dependence is a particularly important issue for SCI applications of ADS, since motor cortex outputs influence spinal cord neurons via various descending pathways (e.g., corticospinal, cortico-reticulospinal) with different conduction velocities and multiple synaptic connections. Our hypothesis is that, several weeks after SCI, the synaptic efficacy of spared descending pathways from motor cortex to spinal cord can be strengthened by using ADS to replicate the natural timing of pre- and post-synaptic events, resulting in an increase in cortically evoked-activity in the hindlimb spinal cord.

A similar ADS approach was used by Zimmermann and Jackson in two monkeys with temporary inactivation of primary motor cortex. In that study, cortical spikes generated in premotor cortex were used to trigger electrical stimulation in the cervical spinal cord, resulting in restoration of hand function during the closed-loop stimulation (Zimmermann and Jackson, 2014). In the present study, we sought to extend these findings to a model of hindlimb spinal cord injury.

Previously, we demonstrated that a lower thoracic spinal cord contusion injury that damaged the corticospinal tract drastically altered the timing of spike events in the spinal cord that were evoked by hindlimb motor cortex stimulation. Long-latency spikes (~20-40 ms) and EMG activity were abolished, while short-latency spikes (~10 ms) persisted. This suggests that after damage to the corticospinal tract, the hindlimb motor cortex can still provide control signals for spinal cord neurons via various spared polynsynaptic routes. Those results provided the basis for the present study examining the ability of ADS with two different cortical spike-ISMS delays (10 and 25 ms) to enhance the cortical modulation of spinal cord neurons. The results demonstrate that ADS strengthens the synaptic efficacy of spared descending pathways after lower thoracic contusion injury, but that different populations of spinal cord neurons are differentially strengthened by the two time delays. To our knowledge the present study is the first to

employ cortical spike driven intraspinal microstimulation in an SCI model, and provides further support for the therapeutic use of ADS after SCI.

Methods

Subjects

Thirty-four adult, male, Sprague Dawley rats were used in this study. Body weights ranged from 356—486 g (411.1 ± 29.8 g) and ages ranged from 90—105 days old (96.0 ± 4.0 days old) at the time of the electrophysiological experiments. Each rat underwent a surgical procedure to induce a spinal cord contusion injury at T8. Four weeks later, rats underwent neurophysiological procedures to examine the effects of two ADS stimulation parameters: 1) The time delay between recorded action potentials (i.e., spikes) in the motor cortex hindlimb area (HLA) and onset of intraspinal microstimulation (ISMS) in the ventral horn of the lumbar spinal cord (10 or 25 ms) and 2) the number of biphasic ISMS pulses (1 or 3). Ten rats were removed from the study due to adverse surgical complications. Thus, 24 rats were randomly assigned to one of four ADS parameter groups and completed the study: 1) *Group 10ms_1P* (n = 7): 10 ms time delay with 1 ISMS pulse; 2) *Group 10ms_3P* (n= 5): 10 ms time delay with 3 pulses; *Group 25ms_1P* (n = 7) 25 ms time delay with 1 pulse; and *Group 25ms_3P* (n = 5): 25 ms time delay with 3 pulses. All procedures were performed in accordance with the *Guide for the Care and Use of Laboratory Animals* (Institute for Laboratory Animal Research, National Research Council, Washington, DC: National Academy Press, 1996). The protocol was approved by the University of Kansas Medical Center Institutional Animal Care and Use Committee.

General Surgical Procedures

In each rat, two surgical procedures were performed: 1) a recovery surgical procedure to induce a contusion SCI and 2) a terminal procedure to a) implant microelectrodes into hindlimb motor cortex and spinal cord, b) implant EMG electrodes into selected hindlimb muscles, and c) conduct ADS neurophysiological sessions (Figure 1). In both surgical procedures, after a stable anesthetic state was reached using isoflurane anesthesia, ketamine hydrochloride (100 mg kg^{-1}; IP)/xylazine (5 mg kg^{-1}; IP)

was delivered. Anesthesia was maintained with subsequent doses of ketamine (0.1 mL; IP or IM) and monitored via pinch and corneal responses. Additional doses of ketamine were administered if the rat reacted to a pinch of the forepaw/hindpaw or blinked after lightly touching the cornea. Aseptic conditions were maintained for both procedures.

Spinal cord injury (SCI)

All animals underwent a T8 laminectomy and moderate contusion injury using an Infinite Horizon spinal cord impactor (Precision Systems and Instrumentation, LLC, Fairfax Station, VA) with 175 kDyn impact. Displacement distance reported by the impactor software for each contusion was recorded at the time of surgery and was used as an initial quantitative marker for successful impact. The average displacement value of the impactor was 1000.4 ± 123.8 µm (mean ± SD) from the surface of the spinal cord. At the conclusion of the surgery, 0.25% bupivacaine HCl was applied locally to the incision site. Buprenex (0.01 mg kg^{-1}; SC) was administered immediately after surgery and 1 day later. All animals were monitored daily until the end of the experiment. On the day of surgery, and for 1-week post-surgery, the rats received a daily SC injection of 30,000 U of penicillin (Combi-Pen 48) in 5 mL of saline to prevent infections and dehydration. Rats' bladders were expressed twice-daily until animals recovered urinary function. From the second week onward, animals were supplemented with vitamin C pellets (BioServ, Frenchtown, NJ) to avert urinary tract infection (Behrmann et al., 1992).

BBB Scoring

Locomotor performance was assessed using the Basso, Beattie, and Bresnahan (BBB) scale (Basso et al., 1995). BBB scoring was performed before SCI and once per week for up to 4 weeks post-SCI. Four weeks was chosen because BBB scores typically plateau by 4 weeks and behavior is relatively stable (Scheff et al., 2003; Krizsan-Agbas et al., 2014). A straight walkway was utilized for the testing. Rats were habituated to the apparatus for 1 week prior to BBB scoring. A BBB score of 13-15 at 4 weeks

post-SCI was set as the inclusion criterion for this study; however, no rats were removed from this study due to this criterion.

Neurophysiology procedures.

Experimental design. Neurophysiological sessions were conducted four weeks after SCI. Spike-stimulus conditioning (i.e., ADS) was conducted in three, 1-hour ADS conditioning bouts for a total of 3 hours of ADS. Changes in synaptic efficacy were inferred by comparing spikes evoked by ICMS during a 5 min baseline period before ADS and three 5 min test periods following each ADS bout (Figure 1).

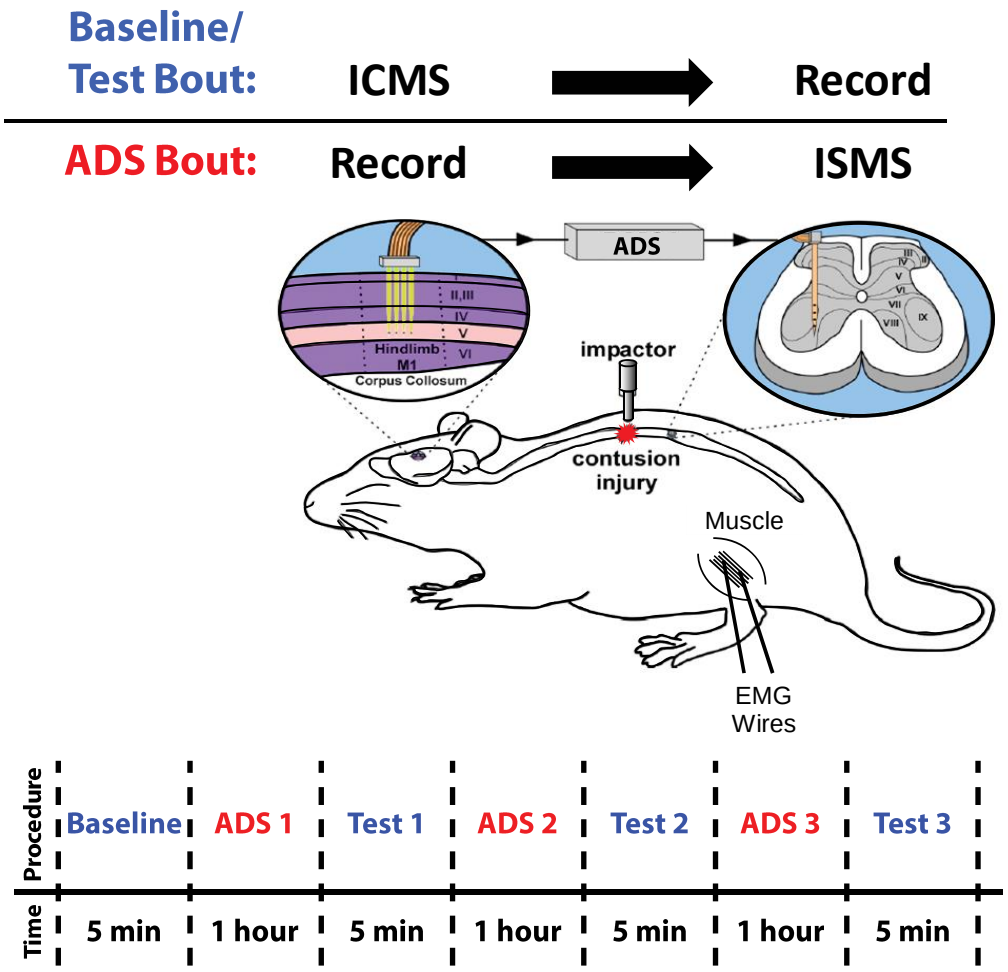

Figure 1. Overview of Experimental Design. Baseline/Test Bout: ICMS was applied to hindlimb motor cortex (HLA) while evoked spikes were recorded from spinal cord neurons below the level of a T8 contusion injury. **ADS Bout:** Spikes from HLA were recorded and used to trigger ISMS in the ventral horn of the thoracic spinal cord below the level of the injury. **ADS Timeline:** ADS bouts were conducted in one-hour sessions for a total of three hours. Test bouts were 5 min in duration, conducted at baseline and after each hour of ADS.

EMG fine-wire electrode implantation. The implantation and verification of fine-wire EMG electrodes into hindlimb muscles was conducted as previously described (Borrell et al., 2017). EMG electrodes were implanted in four hindlimb muscles: the lateral gastrocnemius (LG), tibialis anterior (TG), vastus lateralis (VL), and biceps femoris (BF). Each EMG electrode consisted of a pair of insulated multi-stranded stainless-steel wires exposed approximately 1 mm, with the exposed, implanted end of the wire folded back on itself ('hook' electrode). Implantation locations were determined by surface palpation of the skin and underlying musculature. Once the hindlimbs were shaved, EMG electrodes were inserted into the belly of each muscle with the aid of a 22-gauge hypodermic needle. For each EMG electrode pair, wires were positioned approximately 5 mm apart in each muscle. The external portion of the wires was secured to the skin with surgical glue (3M Vetbond Tissue Adhesive, St. Paul, MN) and adhesive tape. An additional ground lead was placed into the base of the tail.

To verify that the EMG electrodes were within the belly of the muscle, a stimulus isolator (BAK Electronics, Inc., Umatilla, FL) was used to deliver a biphasic (cathodic-leading) square-wave current pulse to the muscle through the implanted EMG electrodes. In addition, the impedance between the EMG electrodes was tested via an electrode impedance tester (BAK Electronics, Inc., Umatilla, FL). The EMG electrodes were determined to be inserted properly and within the desired muscle if: a) the electrode impedance was approximately 7-8 kΩ; b) direct current delivery to the muscle resulted in contraction of the desired muscle, and c) the movement threshold was ≤ 5mA.

Identification of motor cortex HLA. The rats were placed in a Kopf small-animal stereotaxic frame (David Kopf Instruments®, Tujunga, CA) and the incisor bar was adjusted until the heights of

lambda and bregma were equal (flat skull position). The cisterna magna was punctured at the base of the skull to reduce edema during mapping. A craniectomy was performed over the motor cortex. The general location of the craniectomy was guided by previous motor mapping studies in the rat (Frost et al., 2013; Frost et al., 2015). The dura over the cranial opening was incised and the opening was filled with warm, medical grade, sterile, silicone oil (50% Medical Silicone Fluid 12,500, 50% MDM Silicone Fluid 1000, Applied Silicone Corp., Santa Paula, CA) to prevent desiccation during the experiment.

A magnified digital color photograph of the exposed cortex was taken through a surgical microscope. The image was transferred to Canvas 3.5 where a 200 µm grid was superimposed, by calibration with a millimeter ruler, to indicate intended sites for microelectrode penetration. ICMS was conducted in the HLA of the primary motor cortex (M1) to verify the topographic location (Figure 2A). In SCI rats, hindlimb movements cannot be elicited with ICMS from HLA. Thus, an indirect approach was taken to assure that the cortical microelectrodes were located in HLA. First, the general location of the HLA can be predicted based on stereotaxic coordinates from previous ICMS studies in healthy rats (Frost et al., 2013). Further, hip movements are consistently evoked immediately caudal to the forelimb area (blue dots in Figure 2A) and lateral to the trunk area (light blue dots in Figure 2A). In SCI rats, ICMS can evoke forelimb and trunk movements (Frost et al., 2015).

ICMS was delivered to the ventral-most site on a single-shank Neuronexus probe (Neuronexus, Ann Arbor, MI) positioned at regularly spaced sites on the superimposed 200 µm grid. Each electrode site used for stimulation was iridium activated and had an impedance in the range of ~50-70 kΩ with a surface area of 1250 μm^2. The maximum compliance voltage of the system was 24 V. Electrode depth was controlled using a Kopf hydraulic microdrive (Kopf Instruments, Tujunga, CA) and reached ~1700 µm (i.e., Layer V of the cortex). The stimuli consisted of thirteen, 200 µs biphasic cathodal pulses delivered at 300 Hz repeated at 1/sec from an electrically isolated, charge-balanced (capacitively coupled) stimulation circuit. A maximum current of 100 µA was used during ICMS mapping.

Identification of lumbar spinal cord. Following ICMS mapping, a midline incision was made, exposing the T12-L2 vertebrate. A laminectomy was performed on the T13-L1 vertebrae exposing the L2-S1 segments of the spinal cord. The dura mater was removed using fine forceps and small scissors to allow electrode penetration. Animals were stabilized with a custom rodent spinal fixation frame (Keck Center for Collaborative Neuroscience Rutgers, The State University of New Jersey, USA) attached to the dorsal processes of vertebrae T12 and L2.

Previously derived 3-dimensional ISMS-evoked topographic maps were used in the guidance of stimulation sites in the hindlimb spinal cord (Borrell et al., 2017). A similar 200 µm grid was placed over a digital photomicrograph of the spinal opening for the mapping of evoked movements (Figure 2B). Stimulation sites were located ~0.8 mm lateral to the central blood vessel (i.e., midline) on the right side of the spinal cord and at a depth ~2.27 mm below the surface of the spinal cord (i.e., in the ventral horn). ISMS stimuli consisted of three 200 µs biphasic cathodal pulses delivered at 300 Hz repeated at 1/sec. ISMS-evoked movement threshold was measured during ISMS mapping and recorded as the lowest current level (i.e., increments of 1 µA) needed to evoke a consistent, repetitive joint displacement.

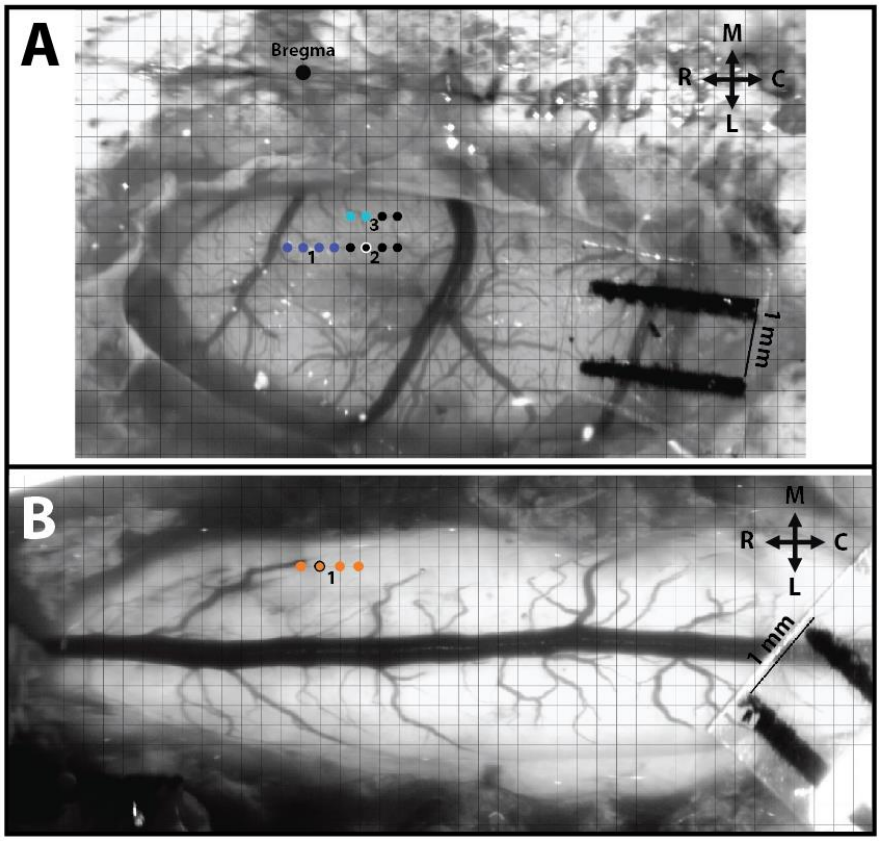

Figure 2. Intracortical and intraspinal microstimulation mapping and site pairing conducted in SCI rats. **A)** Hindlimb motor cortex with superimposed grid for ICMS mapping. The large black dot is at Bregma, the dark blue dots represent stimulation sites that resulted in ICMS-evoked forelimb movements, the light blue dots represent evoked trunk movements, and the small black dots represent sites of no evoked movement. **B)** Hindlimb spinal cord with superimposed grid for ISMS mapping. Each orange dot represents a stimulation site that resulted in ISMS-evoked hindlimb movement. The orange dot with the black outline represents the site of an ISMS-evoked hip movement paired for ADS. R = Rostral, C = Caudal, M = Medial, and L = Lateral.

Intracortical and intraspinal evoked movement site matching. After ICMS was used to define forelimb and trunk sites, as well as non-responsive sites, a putative hip site (black dot with white outline in Figure 2A) was located. For subsequent ADS and test bouts, this site was paired with an ISMS-evoked hip site in the lumbar spinal cord (orange dot with black outline in Figure 2B).

ICMS-evoked spike recordings (Baseline and Test Bouts). Using the paired sites of the HLA and hindlimb spinal cord, a stimulating electrode was inserted into the HLA and a recording microelectrode was simultaneously inserted in the hindlimb spinal cord site. The recording microelectrode was a single-shank, 16-channel Michigan-style linear microelectrode (Neuronexus, Ann Arbor, MI). Each of the 16

sites had a site area of 703 μm^2, separation of 150 µm, thickness of 15 µm in diameter, and impedance of ~0.3 MΩ. The tip of the electrode was lowered to a depth of ~2270 µm below the spinal cord surface. ICMS was used to test corticospinal coupling by delivering a test stimulus in HLA, and ICMS-evoked spikes were recorded from the spinal cord and EMG from the hindlimb muscles. For baseline and test bouts, the ICMS stimulus consisted of three, 200 µs biphasic cathodal pulses delivered at 300 Hz repeated at 1/sec, and an ICMS intensity of 100 µA was used for all baseline and test bouts. During each baseline and test bout, neural and EMG activity were recorded and digitized for ~5 min from each of the 16 active recording sites and four fine-wire pairs, respectively, using neurophysiological recording and analysis equipment (Tucker Davis Technologies, Alachua, FL).

Activity-dependent-stimulation (ADS) paradigm. Using the paired HLA and spinal cord hip sites, the recording microelectrode was inserted into the HLA site and the stimulating microelectrode was inserted into the hindlimb spinal cord site. The stimulating microelectrode was positioned at ~2.27 mm below the surface of the spinal cord (i.e., in lamina VIII/IX in the ventral horn), as the long-range therapeutic goal is to enhance cortical modulation of spinal motor neurons. Using principal component analysis (Lewicki, 1998), spikes were recorded and sorted in real-time from a single channel in HLA and used to trigger stimulation in the paired site in the hindlimb spinal cord. The triggered ISMS stimulus consisted of one or three, 200 µs biphasic cathodal pulses delivered at 300 Hz repeated at 1/sec. The stimulus intensity for ADS was set at 50% of the ISMS movement threshold in each rat to reduce the possibility of evoked movements during ADS therapy and to eliminate the possibility of fatigue on the muscle.

The ADS parameters of interest were time delay between recorded cortical spike and spinal cord stimulation and the number of ISMS pulses. Delays of 10 and 25 ms between recorded HLA spike and triggered stimulus pulse(s) were chosen based on natural response times observed in previous experiments (Borrell et al., 2020). Briefly, ICMS-evoked spiking activity in the hindlimb spinal cord was

consistently observed with a 10 ms latency in healthy rats, hence a 10 ms time delay was chosen. A 25 ms time delay was chosen because it matched the latency of ICMS-evoked hindlimb EMG activity in healthy rats.

Three-pulse trains are typically used to evoke EMG activity and joint movements elicited by ISMS (Moritz et al., 2007). However, to document ISMS-evoked EMG activity more precisely, and to minimize polysynaptic effects, ADS effects were also tested using only one pulse as the ISMS stimulus.

Neurophysiological data analysis

Spike sorting during baseline and test bouts. Neural spikes were discriminated offline with OpenSorter software (Tucker Davis Technologies, Alachua, FL) using principal component analysis (Lewicki, 1998). ICMS-evoked activity recorded during the baseline and test bouts from each channel in the hindlimb spinal cord was represented in post-stimulus spike histograms for 200 ms around the onset of each ICMS stimuli (ICMS begins at 0 ms; histogram extends -100 ms before and +100 ms after onset ICMS) using custom software (Matlab; The Mathworks, Inc., Natick, MA). Spiking activity was averaged into 1 ms bins over the ~5 min recording (i.e., averaged over ~300 ICMS trains). Spike activity could not be discriminated during the first 7 ms after the onset of the ICMS train due to the stimulus artifact.

For analysis of spiking responses during the baseline and test bouts, the 16 recording channels in the hindlimb spinal cord were divided into four dorsoventral sectors based on depth below the surface of the spinal cord. The dorsoventral sectors (Figure 3) were: Dorsal Sector (720—1020 mm; dorsal horn), Upper Intermediate Sector (1120—1420 mm; intermediate layer), Lower Intermediate Sector (1520—1820 mm; intermediate layer), and Ventral Sector (1920—2220 mm; ventral horn).

Firing rate (FR) calculation. The ICMS-evoked firing rate (FR) (i.e., total number of recorded spikes per 1ms bin/total time of recording) was calculated for each time bin of the post-stimulus spike histograms using custom software (Matlab; The Mathworks, Inc., Natick, MA). The FR was only

considered for analysis if the FR for the respective time bin was greater than 2x standard deviation (horizontal, dashed, red line of Figure 7) above the average FR pre-ICMS (horizontal, solid, red line of Figure 6). Pre-ICMS FR was derived by averaging the FR of each time bin 10 ms before the onset of ICMS (i.e., from -10 to 0 ms in the post-stimulus spike histogram).

To narrow the range of potential cortical spike-ISMS delays, we utilized data from a previous study wherein we determined the latencies of ICMS-evoked action potentials in lower thoracic spinal cord neurons in healthy and SCI rats (Borrell et al., 2020). In healthy rats, ICMS-evoked spikes in the lower thoracic spinal cord occurred during a narrow, short-latency period (10-12 ms) as well as at longer latencies that formed a broader distribution (~20-40 ms). ICMS-evoked EMG activity was observed at ~25-28 ms post-ICMS. In SCI rats, ICMS-evoked spikes below the level of the SCI were found consistently at short latency (~10-12 ms). However, at the longer latencies, FR was substantially lower after the SCI, and only a few bins displayed FR significantly above baseline. Based on these previous results, in the present study, the maximum FR was defined for the short-latency period (10-12 ms post-onset ICMS) and the long-latency period (24-36 ms). Then, the mean FR and standard error for the short- and long-latency periods were calculated for each baseline/test bout in each rat, and in each dorsoventral sector.

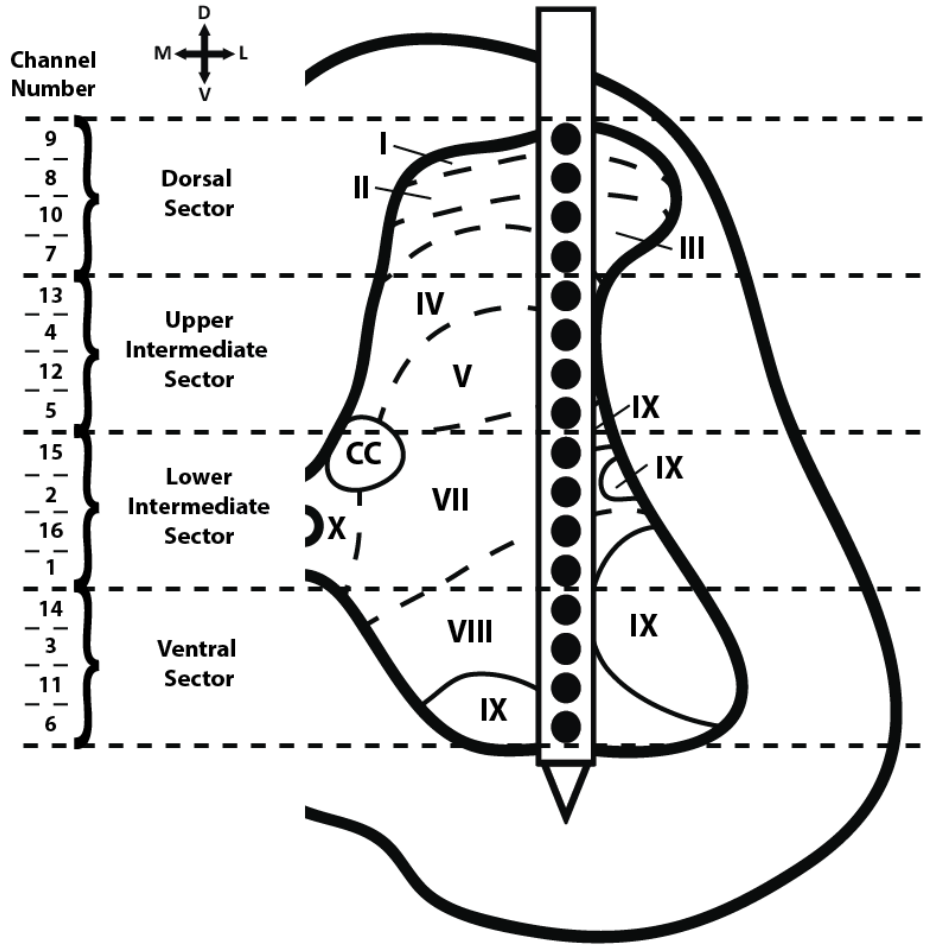

Figure 3. Cross-sectional schematic diagram of hindlimb spinal cord with placement of the recording electrode during the baseline and test bouts. The channel numbers of the recording sites in each of the four dorso-ventral sectors are shown at the left. Previous topographical studies indicate the rostral sector of vertebrae T13 of the Sprague Dawley rat is located at spinal cord segmental level L2-L3 (Gilerovich et al., 2008). Thus, the recording electrode was located in segmental level L2-L3. Based on cytoarchitectonic organization in the rat, electrode sites were in or near all laminae except for laminae VI (seen only in L3-S1 segments of the rat) and laminae X (found medially around the central canal)(Molander et al., 1984).

Stimulus-triggered average (StTA) of EMG. Using custom software (Matlab; The Mathworks, Inc., Natick, MA), StTAs of rectified EMG from leg muscles were plotted to determine muscle activation (Hudson et al., 2015; Borrell et al., 2017). For each of the implanted muscles, EMG data were recorded for at least 10 stimulus trains during ICMS and ISMS procedures at movement threshold or a maximum current of 100 µA and averaged over a time window of 220 ms. StTAs were aligned to the time of the

first stimulus (i.e., 0 ms) and included data from -20.2 to +199.9 ms relative to the time of the first stimulus. A muscle was considered active when the average rectified EMG reached a peak ≥ 2.25 SD above baseline values in the interval from -20.2 to 0 ms and had a total duration of ≥ 3 ms. The stimulus artifact was minimal to absent in EMG recordings with no muscle activation. If an artifact was observed, the amplitude of the artifact was minimal compared to the amplitude of the evoked movement; however, the averaging of the StTAs of EMG recordings largely eliminated the stimulus artifact. As a result, the stimulus artifact was determined to have minimal to no effect on the recordings. EMG potentials were high- and low-pass filtered (30 Hz-2.5 kHz), amplified 200-1000 fold, digitized at 5 kHz, rectified and recorded on an RX-8 multi-channel processor (Tucker-Davis Technology, Alachua, FL).

Statistical analyses

Statistical analyses were performed using JMP 11 software (SAS Institute Inc., Cary, NC) and followed the rationale of a comparable study (Averna et al., 2019). The current study was designed to assess the effect and interactions of various ADS parameters in separate dorsoventral sectors over time on neuronal activity. Since the independence of individual neuron firing rates cannot be assumed within a particular rat and because the distribution of firing rates tends to have a Poisson distribution with a long tail (and thus, not normally distributed), a generalized linear mixed model (GLMM) for repeated measures was used. GLMM is a powerful statistical tool that permits modeling of not only the means of the data (as in the standard linear model) but also their variances as well as within-subject covariances (i.e., the model allows subjects with missing outcomes—unbalanced data—to be included in the analysis). Thus, data are presented as average ± standard error of the mean unless otherwise stated, and p-values < 0.05 were considered significant.

Histology

At the end of each experiment, animals were euthanized with an intraperitoneal injection of sodium pentobarbital (Beuthanasia-D; 100 mg kg^{-1}) and transcardially perfused with 4% paraformaldehyde in 0.1 M PBS. The spinal cord was sectioned at 30 µm on a cryostat in the coronal plane. Histology was performed on selected sections with cresyl violet stain for Nissl bodies to verify the injury.

Results

BBB Scores

Each rat scored 21 on the BBB scale (normal) before SCI. At 1-week post-SCI, BBB scores were significantly lower relative to baseline (Table 1; $p < 0.0001$). BBB scores improved over subsequent weeks but remained significantly lower relative to baseline at 4 weeks post-SCI (Table 1; $p < 0.0001$). There was no statistical difference in BBB scores between groups for any week ($p > 0.05$). At 4-weeks post-SCI, BBB scores confirmed that rats had consistent weight-supported plantar steps, no or occasional toe clearance (i.e., scraping of the digits on the ground) during forward limb advancement, consistent forelimb-hindlimb coordination, and predominant paw position during locomotion that was always rotated externally just before it lifted off at the end of stance and either externally rotated or parallel to the body at initial contact with the surface.

Table 1. Mean BBB score at baseline and at weeks 1-4 post-SCI and displacement of impactor at time of SCI for each rat group and all rats combined. There was no statistical difference in impactor displacement at SCI nor in BBB scores between groups at any of the four weeks ($p > 0.05$). ***** = Significant difference of BBB score when compared to baseline (within-group comparison; $p < 0.0001$).

Group	Displacement at SCI (µm)	BBB Scores (Mean ± SD)				
		Baseline	Week 1	Week 2	Week 3	Week 4
10ms_3P	1057.8 ± 94.5	21.0 ± 0.0	10.8 ± 1.3*	12.0 ± 1.4*	13.0 ± 1.6*	13.4 ± 0.9*
25ms_3P	937.8 ± 251.2	21.0 ± 0.0	11.0 ± 3.4*	13.2 ± 4.4*	14.0 ± 3.5*	14.8 ± 1.5*
10ms_1P	997.3 ± 47.7	21.0 ± 0.0	10.1 ± 2.3*	11.9 ± 2.5*	13.7 ± 2.4*	14.1 ± 1.7*
25ms_1P	1007.3 ± 49.1	21.0 ± 0.0	12.4 ± 2.4*	14.3 ± 1.6*	14.4 ± 2.1*	14.9 ± 1.7*
Overall	1000.4 ± 123.8	21.0 ± 0.0	11.1 ± 2.5*	12.9 ± 2.7*	13.8 ± 2.4*	14.3 ± 1.5*

SCI Verification

A representative image of a histological section through the injury epicenter is shown in Figure 4. Briefly, the injury spared an outer rim of white matter that surrounded a central core lesion. Remnants of the gray matter were rarely seen at the lesion center.

Figure 4. Representative image of spinal cord injury epicenter 4 weeks after injury stained with a cresyl violet acetate solution.

Spike Frequency in HLA During ADS

The profiles of spikes recorded in HLA and used to trigger stimulation during each hour of ADS remained relatively consistent over the 3-hours of ADS (Figure 5, Left). Additionally, there were no significant changes in the HLA spike frequency in any group after 3 hours of ADS relative to the 1st hour of ADS (Figure 5, Right). While there were minor within-group increases in average spike frequency during the second and third hour of ADS in the 10ms_1P and 25ms_3P groups relative to the first hour of ADS, these increases were not significant. There were minor decreases in average spike frequency during the second and third hour of ADS in the 10ms_3P and 25ms_1P groups relative to the first hour of ADS, but again, these changes were not significant.

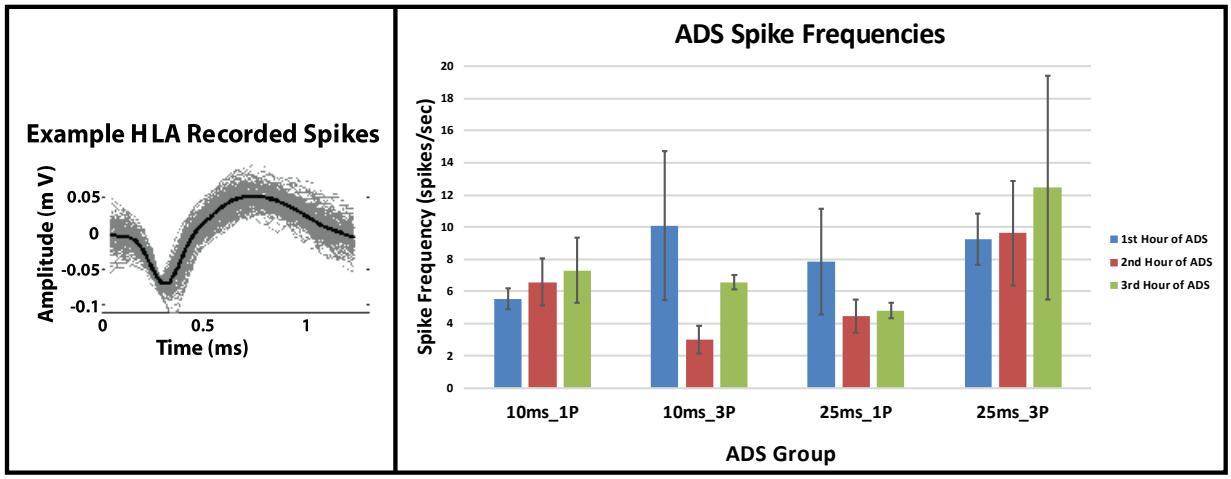

Figure 5. Extracellular spikes recorded in hindlimb motor cortex (HLA) during the ADS sessions. **Left:** Exemplar spike profiles recorded from layer V of hindlimb motor cortex combined from two different rats. These spikes were used to trigger ISMS pulses in the ventral horn of the lumbar spinal cord during ADS. **Right:** Average spike frequencies of recorded spikes for each parameter group during each hour of ADS. Data were derived from 5-minute recordings at the end of each hour of ADS.

ISMS and ICMS Current Intensity

The average ISMS stimulus intensity required to evoke a hindlimb movement (movement threshold) during spinal cord mapping was 9.00 ± 5.90 µA. There was no statistical difference in ISMS movement threshold intensities between groups (Table 2; $p > 0.05$).

The average ISMS intensity used for ADS bouts was 4.50 ± 2.95 µA (i.e., ADS intensity). There was no statistical difference in ISMS intensity during ADS bouts between groups (Table 2; $p > 0.05$).

Since movement could not be evoked during ICMS mapping in SCI rats, a fixed intensity of 100 µA was used for ICMS during the 5-minute baseline and test bouts. The average ISMS stimulus movement thresholds and ADS stimulus intensities used for each group are shown in Table 2.

Table 2. Mean and standard deviations at four weeks post-SCI during the ADS procedure. ISMS threshold was recorded during ISMS mapping at movement threshold. ADS intensity was 50% of ISMS threshold. ICMS intensity was set at 100 µA and used during the 5-minute baseline and test bouts.

Group	ISMS Threshold (µA)	ADS Intensity (µA)	ICMS Intensity (µA)
10ms_1P	7.14 ± 2.27	3.57 ± 1.13	100.00 ± 0.00
25ms_1P	8.86 ± 5.98	4.43 ± 2.99	100.00 ± 0.00
10ms_3P	10.80 ± 8.79	5.40 ± 4.39	100.00 ± 0.00
25ms_3P	10.00 ± 7.07	5.00 ± 3.54	100.00 ± 0.00
Combined	9.00 ± 5.90	4.50 ± 2.95	100.00 ± 0.00

EMG Activity

ICMS-evoked EMG activity was never observed before or after ADS (i.e., during baseline and test bouts, no EMG potentials were greater than two standard deviations above the baseline EMG activity). During ADS, ongoing EMG amplitude fluctuated periodically, but no consistent changes were evident. The following qualitative observations (and their incidence) are of note: 1) EMG activity was present in each hindlimb muscle and EMG amplitude increased over the 3 hours of ADS (n = 6 instances), 2) EMG activity was present during the 1st hour of ADS but was not present after the 2nd or 3rd hour of ADS (n = 3 instances), 3) EMG activity was never present over the 3 hours of ADS (n = 10 instances), and 4) EMG activity increased during the 2nd hour of ADS but was not present after the 3rd hour of ADS (n = 1 instance). These observations did not occur systematically and thus the data were not analyzed further.

Post-stimulus spike histograms

The ICMS-evoked spiking activity was recorded for each channel and analyzed over four dorsoventral sectors delineated by depth below the surface of the spinal cord. After 3 hours of ADS, post-stimulus spike histograms from the 10ms_1P group (Figure 6) showed qualitatively that ICMS-evoked spiking activity increased at a latency of ~10 ms from onset of ICMS (i.e. 0 ms), especially within the ventral sector.

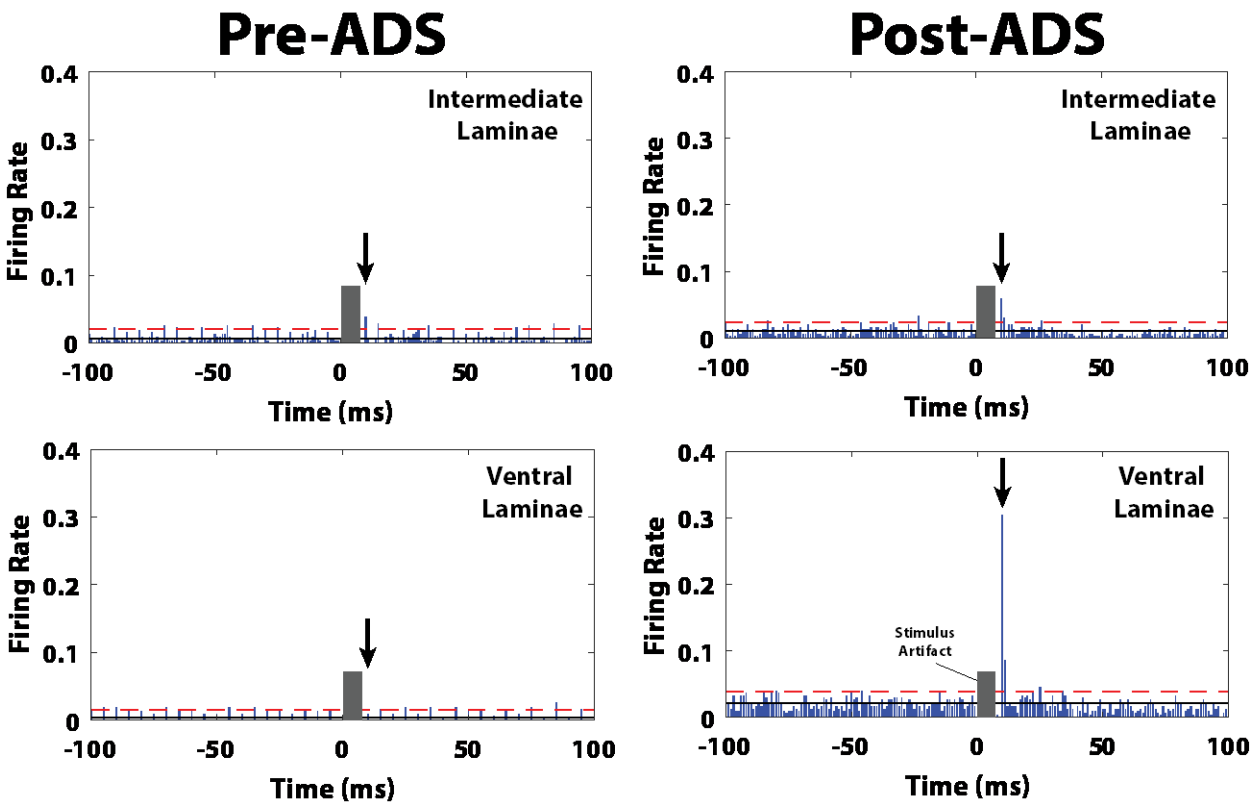

Figure 6. Post-stimulus spike histograms from rats in the 10ms_1P group before and after 3 hours of ADS. Post-ICMS spikes occurred during a short latency period from 10-12 ms, and a long-latency period from 24-36 ms. Black arrow indicates the short-latency bin with the highest ICMS-evoked FR, and thus used for pre/post ADS comparison. The number of recorded ICMS-evoked spikes during the short-latency period increased in the ventral laminae (lower right) after 3 hours of ADS. Solid black line is average FR before onset ICMS (i.e., pre-ICMS FR). Red dashed line is 2x standard deviations above pre-ICMS FR.

ICMS-Evoked Maximum Firing Rate at Short Latency

Maximum FR (hereafter, simply called FR) during the short-latency period typically occurred at 10 ms (all test bouts; mean ± SE = 10.34 ± 0.07 ms; median = 10.00 ms), but occasionally at 11 and 12 ms. There were no statistical differences in latency after ADS bouts compared with baseline. In each of the four groups, FR increased in one or more dorosoventral sectors of the cord after ADS compared with baseline FR (Figure 7).

In the Dorsal sector, FR increased significantly after 2 and 3 hours of ADS in the 25ms_3P group ($p = 0.0449$; $p = 0.0050$). An increase after 1 hour was also seen in the 10ms_3P group ($p < 0.0001$), but this increase was not sustained after 2 or 3 hours.

In the Upper Intermediate sector, FR increased significantly after 2 and 3 hours of ADS in the 10ms_1P group ($p = 0.0022$; $p = 0.0211$) and the 25ms_3P group ($p = 0.0003$; $p = 0.0005$). There was also an increase after 3 hours in the 25ms_1P group ($p = 0.0011$).

In the Lower Intermediate sector, FR increased significantly after 3 hours in the 25ms_1P group ($p = 0.0002$). FR also increased significantly after 2 hours in the 25ms_3P group ($p = 0.0226$), but this increase was not sustained at 3 hours.

Finally, FR increased in the Ventral sector after 2 and 3 hours of ADS in the 10ms_3P group ($p = 0.0158$; $p = 0.0120$) and in the 25 ms_1P group ($p = 0.0415$; $p = 0.0139$). FR also increased significantly after 3 hours in the 10ms_1P group ($p = 0.0057$).

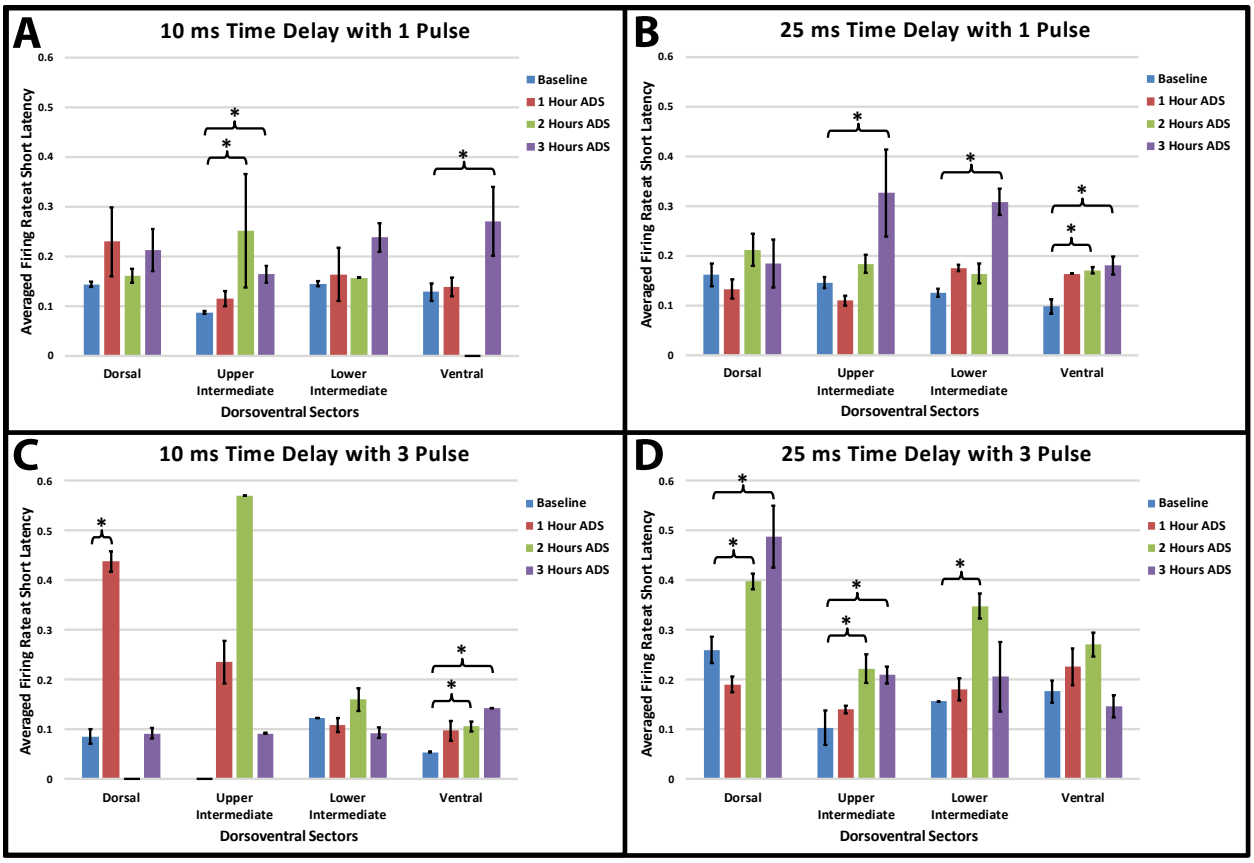

Figure 7. Maximum ICMS-evoked firing rates (i.e., means ± std err) during the short-latency period for each dorsoventral sector at baseline and after each hour of ADS. Generally, the 10 ms post-ICMS bin was used for this analysis. **A)** 10ms_1P ADS group, **B)** 25ms_1P ADS group, **C)** 10ms_3P ADS group, and **D)** 25ms_3P ADS group. * = Significant increase in maximum firing rate when compared to baseline recordings ($p < 0.05$).

ICMS-Evoked Maximum Firing Rate at Long Latency

Maximum FR during the long-latency period occurred at about 25 ms (all test bouts; mean ± SE = 24.88 ± 0.65 ms; median = 25.00 ms). There were no statistical differences in latency after ADS bouts compared with baseline. As in the short latency period, in each of the four groups, FR increased in one or more dorsoventral sectors of the cord after ADS compared with baseline FR (Figure 8).

In the Dorsal sector, FR increased significantly after 2 and 3 hours of ADS in the 10ms_1P group ($p = 0.0002$; $p < 0.0001$). An increase after 2 hours was also seen in the 25ms_1P group ($p = 0.0048$), but

this increase was not sustained after 3 hours. In the 25ms_3P group, there was an increase in FR after 1 ($p = 0.0150$) and 2 hours ($p < 0.0001$) of ADS, but not after 3 hours.

In the Upper Intermediate sector, FR significantly increased after 2 and 3 hours in the 10ms_1P group ($p = 0.0183$; $p = 0.0108$), and after 1, 2 and 3 hours in the 25ms_3P group ($p = 0.0337$; $p < 0.0001$; $p < 0.0001$).

In the Lower Intermediate sector, FR significantly increased after 1, 2 and 3 hours in the 25ms_1P group ($p = 0.0079$; $p = 0.0083$; $p = 0.0099$), after 2 and 3 hours in the 25ms_3P group ($p = 0.0005$; $p = 0.0248$), and after 3 hours in the 10ms_1P group ($p = 0.0153$).

Finally, in the Ventral sector, FR significantly increased after 2 and 3 hours in the 10 ms_1P group ($p = 0.0136$; $p < 0.0001$), after 3 hours in the 10ms_3P group ($p = 0.0354$), and after 1, 2 and 3 hours in the 25ms_1P group ($p = 0.0391$; $p = 0.0004$; $p = 0.0041$).

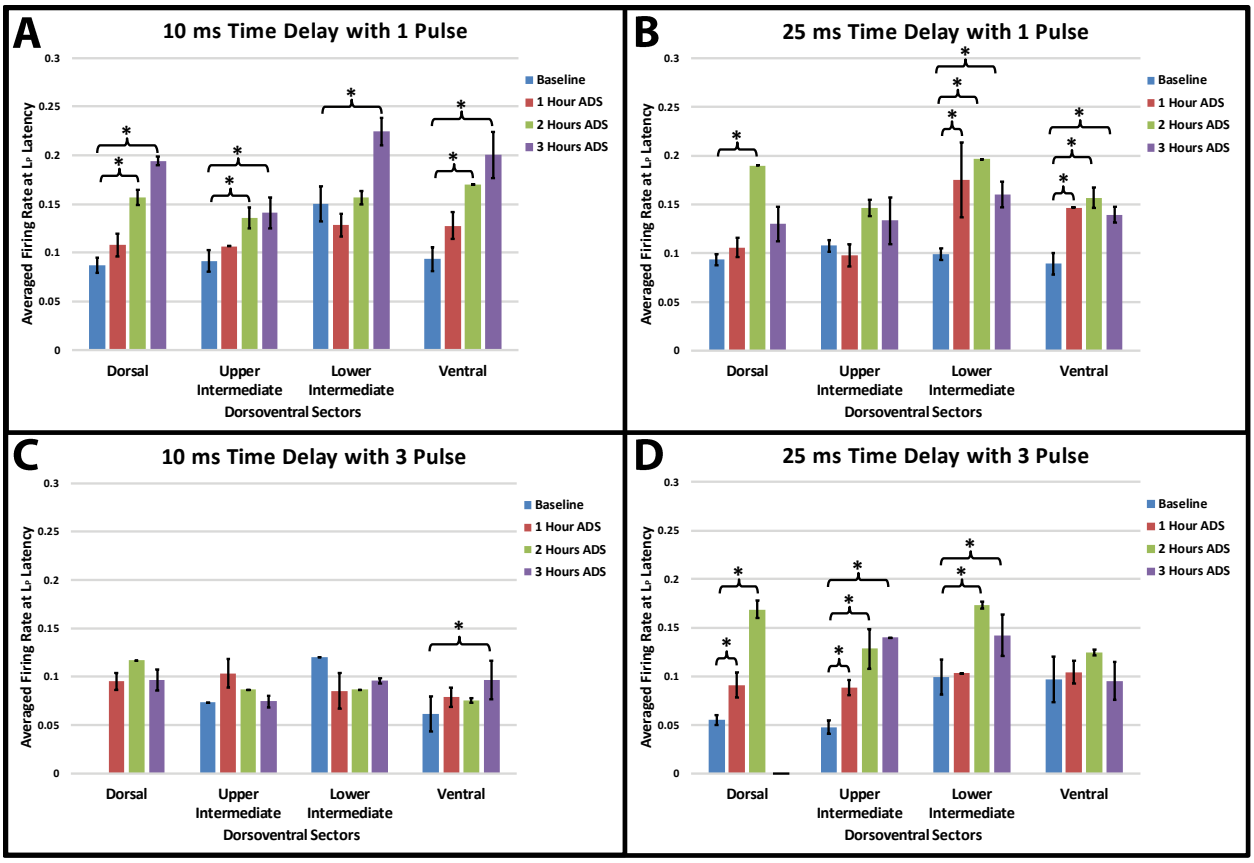

Figure 8. Maximum ICMS-evoked firing rates (i.e., means ± std err) during the long-latency period for each dorsoventral sectors at baseline and after each hour of ADS. Generally, the 24-36 ms post-ICMS bins was used for this analysis. **A)** 10ms_1P ADS group, **B)** 25ms_1P ADS group, **C)** 10ms_3P ADS group, and **D)** 25ms_3P ADS group. * = Significant increase of firing rate when compared to baseline recordings ($p < 0.05$).

ICMS-Evoked Spike Amplitudes

ICMS-evoked spike amplitudes were examined for those spikes occurring within the bins with maximum FR during the short- and long-latency periods, respectively. ICMS-evoked spike amplitudes (Table 3) generally decreased for spikes during both the short- and long-latency periods in most dorsoventral sectors. This was especially evident in all four sectors in the 10ms_1P group at both short and long latencies, and in the 10ms_3P group at long latencies.

Table 3. ICMS-evoked spike amplitudes (mean ± SE) for each ADS group during short- and long-latency periods in each dorsoventral sector before and after each hour of ADS. Grey box and * = Significant difference from baseline recordings in the same dorsoventral sector and ADS rat group ($p < 0.05$).

Table 3.1: ICMS-Evoked Spike Amplitudes (µV) at Short Latency

Rat Group	Dorsoventral Sectors	ADS Time			
		Baseline	1 Hour ADS	2 Hours ADS	3 Hours ADS
10ms_1P	Dorsal	65.1 ± 14.2	**35.7 ± 3.8***	**32.2 ± 2.0***	**35.5 ± 2.5***
	Upper Int.	78.4 ± 12.7	**53.2 ± 6.0***	**44.0 ± 2.9***	**39.9 ± 2.4***
	Lower Int.	106.2 ± 14.8	**54.7 ± 3.1***	**49.4 ± 2.1***	**56.7 ± 3.4***
	Ventral	83.9 ± 14.5	**56.5 ± 4.7***	**59.3 ± 4.3***	**56.2 ± 4.4***
25ms_1P	Dorsal	40.7 ± 3.7	35.0 ± 2.1	33.9 ± 1.6	37.8 ± 3.1
	Upper Int.	53.9 ± 5.3	44.8 ± 3.2	43.9 ± 2.7	39.0 ± 1.7
	Lower Int.	68.0 ± 5.1	60.5 ± 5.2	58.8 ± 4.5	59.3 ± 6.4
	Ventral	59.3 ± 2.9	63.8 ± 9.7	50.5 ± 3.3	48.4 ± 2.2
10ms_3P	Dorsal	45.3 ± 11.0	41.2 ± 4.1	37.5 ± 4.5	21.7 ± 1.3
	Upper Int.	63.7 ± 17.1	50.7 ± 5.8	**42.3 ± 3.4***	38.8 ± 5.4
	Lower Int.	69.3 ± 10.6	60.2 ± 4.8	52.3 ± 6.1	**33.5 ± 5.1***
	Ventral	57.7 ± 10.9	49.6 ± 3.7	49.9 ± 3.7	45.6 ± 7.9
25ms_3P	Dorsal	64.8 ± 9.0	49.1 ± 3.3	46.3 ± 4.4	**37.3 ± 3.4***
	Upper Int.	69.3 ± 7.2	49.4 ± 4.8	53.5 ± 3.9	47.0 ± 4.1
	Lower Int.	69.6 ± 11.3	55.8 ± 3.5	**50.2 ± 2.4***	53.4 ± 4.3
	Ventral	56.5 ± 3.9	65.5 ± 3.5	59.5 ± 5.5	50.0 ± 3.5

Table 3.2: ICMS-Evoked Spike Amplitudes (µV) at Long Latency

Rat Group	Dorsoventral Sectors	ADS Time			
		Baseline	1 Hour ADS	2 Hours ADS	3 Hours ADS
10ms_1P	Dorsal	70.2 ± 16.2	**36.3 ± 3.4***	**35.7 ± 2.8***	**35.0 ± 2.1***
	Upper Int.	82.8 ± 13.2	**47.6 ± 3.9***	**45.0 ± 5.4***	**41.6 ± 1.8***
	Lower Int.	110.1 ± 12.7	**52.4 ± 2.9***	**49.5 ± 1.9***	**54.9 ± 3.3***
	Ventral	80.4 ± 12.0	**53.2 ± 4.0***	**55.7 ± 3.9***	**55.6 ± 4.2***
25ms_1P	Dorsal	41.2 ± 3.3	36.8 ± 2.5	36.3 ± 1.9	40.0 ± 3.3
	Upper Int.	55.1 ± 4.2	44.6 ± 2.8	46.0 ± 2.6	**38.5 ± 1.3***
	Lower Int.	66.6 ± 4.3	59.7 ± 4.8	59.4 ± 3.8	58.7 ± 5.7
	Ventral	56.3 ± 2.9	65.7 ± 9.5	48.8 ± 3.4	51.9 ± 2.0
10ms_3P	Dorsal	80.9 ± 18.0	**46.6 ± 4.8***	**35.7 ± 4.3***	**31.7 ± 4.6***
	Upper Int.	78.4 ± 13.8	**54.6 ± 4.5***	**39.9 ± 3.1***	**39.7 ± 4.4***
	Lower Int.	86.2 ± 13.1	**63.3 ± 4.7***	**46.5 ± 4.2***	**35.0 ± 3.5***
	Ventral	88.3 ± 15.6	**52.8 ± 3.3***	**48.2 ± 3.2***	**50.7 ± 5.5***
25ms_3P	Dorsal	58.5 ± 7.0	47.2 ± 2.9	47.2 ± 4.1	**35.9 ± 2.9***
	Upper Int.	68.3 ± 8.0	52.5 ± 4.5	53.9 ± 3.5	**42.7 ± 3.1***
	Lower Int.	69.1 ± 11.6	57.3 ± 3.8	55.4 ± 2.7	50.4 ± 5.3
	Ventral	57.8 ± 3.0	62.7 ± 3.1	60.1 ± 5.1	53.4 ± 3.3

Discussion

The primary goal of this study was to determine whether activity dependent stimulation (ADS) using different spike-stimulus delays and number of ISMS pulses differentially alters synaptic efficacy in descending motor pathways in an anesthetized rat model of SCI. By pairing sites of similar functional topography in the hindlimb motor cortex and hindlimb spinal cord and synchronizing the delivery of ISMS in the ventral horn with spontaneous neural activity in motor cortex, the synaptic efficacy of descending motor pathways increased, as evidenced by an increase in cortically-evoked spikes in spinal cord neurons at specific post-ICMS latencies. Importantly, efficacy in descending motor pathways was increased throughout four dorsoventral sectors of the hindlimb spinal cord. Here we discuss the likely motor pathways affected by ADS in this study and the functional impact these synaptic efficacy changes could have in motor control.

Spike-Stimulus Delays during ADS are Consistent with STDP-Based Strengthening

In spike timing-dependent plasticity (STDP), the timing between recorded action potentials and triggered stimulation (i.e., ADS) has been shown to determine the polarity and magnitude (i.e., potentiation or depression) of any change in post-synaptic potentials (Markram et al., 1997; Bi and Poo, 1998; Fung et al., 2016). McPherson *et al.* demonstrated that ADS can induce neural plasticity, with a time delay of ~10 ms, that improves behavioral recovery after SCI by synchronizing ISMS below the injury with the arrival of functionally related volitional motor commands signaled by muscle activity in the impaired forelimb (McPherson et al., 2015). The time delays used during ADS in the present study fell within the range of neurophysiologically relevant latencies (i.e., ~25 ms or less), where robust enhancement of synaptic strength was determined in *in vitro* (Feldman, 2012) and *in vivo* (Nishimura et al., 2013) studies.

Short-Latency Neuronal Spikes after Acute ADS

The present results show that after application of ADS, the FR of spinal cord neurons was increased within a short-latency period of 10-12 ms after an ICMS test pulse. The FR increase was observed in all four dorsoventral sectors of the cord. We showed in a previous study that short-latency spikes were still evoked after a moderate spinal cord contusion identical to that used here, and proposed that post-injury spikes were most likely evoked via cortico-reticulospinal fibers (Borrell et al., 2020). This was based on the fast conduction velocities of reticulospinal fibers and the fact that the ventrolateral funiculus, where reticulospinal fibers descend, was spared. Evidence is accumulating that the reticulospinal tract is strongly involved in locomotor coordination in healthy animals (Mitchell et al., 2016) and plays an important role in the initiation and control of open-field locomotion after SCI. For example, it has been shown that after injury, there is a greater recovery of locomotor function with the sparing of reticulospinal fibers (Schucht et al., 2002). Further, spared reticulospinal fibers are known to sprout below an experimental SCI (Ballermann and Fouad, 2006). Thus, it is important to consider the terminations of spared reticulospinal fibers in the context of the present study.

The reticulospinal tract terminates mainly in the intermediate grey matter of lamina VII and VIII in the hindlimb spinal cord of the rat (Matsuyama et al., 1999; Mitchell et al., 2016), which corresponds to the Lower Intermediate sector and part of the Ventral sector of the spinal cord described in the present study. Thus, it is likely that the reticulospinal tract, activated via the spiking neurons in cortex, participated in the ADS-induced increase in FR. Based on depth below the surface of the spinal cord, it was assumed that the stimulating electrode was in lamina VIII or IX (Ventral sector) during ADS, either near spinal cord motor neuron cell bodies, the dendrites of motor neurons (within laminae VIII), or interneurons (laminae VIII). Any increase in FR in the Ventral sector is considered important for functional recovery since it may indicate increased synaptic efficacy in pathways that directly influence motor neurons. The observed increase of FR at short latencies in the Ventral sector was significant after

several post-ADS test bouts whether a 10 ms or 25 ms delay was used. This was expected since both time delays fall within the window of long term potentiation (Bi and Poo, 2001). These time delays also fall within the window for altered cortical output responses when spike-triggered stimulation was used in motor cortex of non-human primates (Jackson et al., 2006). Although a 3-pulse ISMS train (typical protocol for activity-triggered ISMS) is problematic for a simple model of spike-timing relationships, we also observed significant increases in FR in the Ventral sector in the 10ms_3P Group, i.e., when the pulse train spanned approximately 10 – 20 ms after the cortical spike. The only condition where the Ventral sector was not altered significantly was in the 25ms_3P Group, i.e., with ISMS delays ranging from 25 to 35 ms. With long delays and multiple pulses, the synaptic conditioning effects may be compromised since the later pulses fall outside of the optimal window for long term potentiation.

In addition, a large number of reticulospinal fibers also terminate onto long descending propriospinal neurons that mediate the coordination between forelimb-hindlimb and left-right limbs (Frigon, 2017). It has been shown in cats that long descending propriospinal fibers terminate in the lumbosacral region primarily in laminae VII and VIII (Lower Intermediate and Ventral sectors) (Skinner et al., 1980). Thus, the increase in short-latency FR in the Ventral sector (and occasionally in the Lower Intermediate sector) after ADS could also have been mediated by propriospinal fibers activated by the reticulospinal tract.

Finally, there are a smaller number of propriospinal fibers that terminate in laminae I and IV – VI (Dorsal and Upper Intermediate sectors) (Skinner et al., 1980). Assuming these termination patterns are similar in rats and noting the reported conduction velocities of long descending propriospinal neurons to be ~60 m/s (Skinner et al., 1979), polysynaptic connections onto long descending propriospinal pathways could have been activated in chorus with cortico-reticulospinal pathways at the Short latency. The finding that increases in FR in Dorsal and Intermediate sectors generally were more robust with 3 pulses compared with one pulse further supports this polysynaptic hypothesis. Thus, the increased FR at

short-latency seen in the Dorsal and Upper Intermediate sectors after ADS suggests a strengthening of these intact long descending propriospinal pathways via the cortico-reticulospinal tract. Any increase in FR in the Dorsal and Upper Intermediate sectors is considered important for functional recovery since it may indicate increased synaptic efficacy in interneurons that influence the overall neural circuit which indirectly influences motor neurons.

Long-Latency Neuronal Spikes & EMG Activity after Acute ADS

In a previous study, it was shown that the ICMS-evoked long-latency spinal cord spike activity in a healthy, uninjured rat was represented in a broad distribution beginning ~20 ms after ICMS onset, then overlapping with the onset of EMG activity at ~25 ms, and peaking around ~30 ms (median of peak long-latency response, or L_P) (Borrell et al., 2020). After injury, this spiking pattern was disrupted, as the FR at long latencies was reduced substantially, and EMG activity could not be evoked. While FR occasionally rose above baseline, significant spiking was restricted to only one or two millisecond bins within this broad time period. This result was replicated after SCI in the present study, as the FR of long-latency neuronal spikes rose above baseline for only a few time bins within the broad range of 24-36 ms. It was argued in the previous study that the evoked spikes with long latencies were most likely from neurons activated by the corticospinal and (cortico-) rubrospinal tracts due to the known conduction velocities of these tracts. Thus, it is important to consider the terminations of spared corticospinal and rubrospinal fibers in the context of the present study.

The corticospinal tract (CST) terminates mainly in the deep dorsal horn and intermediate grey matter (laminae III – VI) in the hindlimb spinal cord of the rat (Dorsal and Upper Intermediate sectors in present study) but with a few fibers terminating in all dorsoventral sectors (Casale et al., 1988; Akintunde and Buxton, 1992; Mitchell et al., 2016). However, corticomotoneuronal connections are unsupported in rats (Yang and Lemon, 2003; Lemon, 2008). Similarly, the rubrospinal tract (RbST)

primarily terminates in the intermediate grey matter of laminae V, VI, and VII in the rat (Brown, 1974), corresponding to Upper and Lower Intermediate sectors in the present study. Thus, in intact rats, the CST may mediate long-latency spikes in the Dorsal and Upper Intermediate sectors, and the RbST in the Upper and Lower Intermediate sectors. The influence of CST and RbST on spiking in the Ventral sector probably is exerted via interneurons in dorsal and intermediate laminae. In the present study, it is assumed that the CST, descending primarily in the dorsomedial funiculus in the rat, was heavily damaged after the SCI. Thus, any ICMS-driven spikes in the Ventral sector at baseline, and any increases in FR after ADS bouts could have been mediated by polysynaptic activation via spared fiber tracts, including RbST, dorsolateral CST, ventral CST, reticulospinal tract, and vestibulospinal tract.

Similar to the short-latency spikes, ADS resulted in increased FR in the long-latency period for all dorsoventral sectors of the cord. In the Dorsal and Upper Intermediate sectors, FR increases were most prominent in the 10ms_1P Group and the 25ms_3P group. Thus, simple STDP rules regarding optimal spike-stimulus delays do not readily apply. However, these effects were not the result of ISMS alone, since FR increases were not observed in Dorsal and Upper Intermediate sectors in the 10ms_3P Group, and rarely observed in the 25ms_1P Group. This suggests that timing of ISMS pulses relative to activity in motor cortex is critical in driving synaptic plasticity in Dorsal and Upper Intermediate sectors, even at long-latencies.

In the Lower Intermediate sector, FR increases at long-latency were most prominent in the 25ms_1P Group and the 25ms_3P group, i.e., with spike-stimulus latencies that matched the time of the FR increases. Nonetheless, FR increases were also observed in the Lower Intermediate sector in the 10ms_1P group.

Finally, FR increases after ADS were observed in the Ventral sector in all groups except the 25ms_3P group. Even though ADS did not result in re-establishment of ICMS-evoked movement or EMG,

increases in FR of neurons in the vicinity of motor neurons were seen reliably. It can be argued that increased FR in the Ventral horn at long latencies represents the most functionally relevant result in this dataset, since it coincides with the normal timing of neuronal activity in the cord relative to cortical outputs. The motor functionality of the descending motor pathways is dependent on the ability to activate motor neurons that in turn evoke hindlimb muscle activity. As we were unable to evoke any hindlimb movements via ICMS before and after 3 hours of ADS, any increase in synaptic efficacy in the spinal cord induced by ADS was not sufficient to reestablish functional motor outputs, at least not during the 3-hour acute ADS session in anesthetized rats. However, the present study demonstrated that a range of spike-stimulus delays and numbers of stimulation pulses can result in greater responsiveness in neurons within the Ventral sector.

Impact of Acute Plasticity on Recovery

The increased FR of spinal cord neurons in some conditions as early as 1 hour after ADS is a novel and significant finding that may have clinical relevance. These results may drive future electrical stimulation-based therapies. Currently, most electrical stimulation-based therapies are contingent on the maintained delivery of stimulation. The results seen in this study show that enhancement of descending motor pathways can occur after an acute application of ADS therapy. Future studies will have to determine if enhanced synaptic efficacy is maintained post-therapy, the functional significance of this plasticity, its effect on functional motor recovery in the chronic condition, and the potential for behavioral improvement compared to that found after less-invasive electrical stimulation-based therapies.

Possible Suppressive Effect after Acute ADS

The overall decrease of ICMS-evoked spike amplitudes in all ADS rat groups was unexpected. Studies using intracellular recording have reported that excitatory post-synaptic potentials (EPSPs) can

be up- or down-regulated depending on the precise timing of EPSPs with respect to postsynaptic action potentials (i.e., delay/conduction time of neurons between areas of interest) (Markram et al., 1997). Similarly, it has been shown that long-term potentiation or long-term depression can be mediated by the timing of post-synaptic spiking and presynaptic activation (Bi and Poo, 1999). The decrease in ICMS-spiking amplitude after 3 hours of ADS in the present study may be a result of: 1) a weakening of ineffective synapses; 2) the distance between recording site on the electrode and evoked-neuron changed between recordings (i.e., removal and reinsertion of the electrode changed the distance); 3) the damage to the spinal cord due to the removal and reinsertion of the electrode caused the decrease in ICMS-evoked spike amplitude. Overall, it can be assumed that the decrease of ICMS-evoked spike amplitude may be a combination of these reasons. This observed decrease in ICMS-evoked spike amplitudes, in addition to the increase of FR of short- and long-latency neuronal spikes, may suggest that some descending pathways are suppressed while others are strengthened after 3 hours of ADS; however, a simple change in the distance between recording site and evoked neuron during each test bout cannot be ruled out.

Limitations of Study

It is important to note the limitations in the present study. The main technical limitation was the necessity to remove and reinsert the microelectrodes between the 1-hour ADS sessions and the 5-minute test bouts. During ADS, the recording electrode was inserted in the hindlimb motor cortex while the stimulating electrode was inserted in the hindlimb spinal cord. The microelectrodes were then switched during the test bouts (i.e., the stimulating electrode was inserted in the hindlimb motor cortex and the recording electrode was inserted in the hindlimb spinal cord). When removing and reinserting the electrodes, there was a possibility that the microelectrodes were not reinserted into the exact position as before. In addition, there could be neuronal damage with each reinsertion of the electrode.

The ICMS and ISMS mapping did reduce the amount of variation in site location between each ADS session and test bout. The use of two micromanipulators (one for each electrode) also aided with the consistency of electrode insertion and placement on a micron scale. The consistency in recorded HLA spiking profiles over the ADS sessions also indicates that the recording microelectrode inserted in HLA was consistently in the same site each time; however, the change in spike amplitudes of the evoked spikes in the spinal cord may suggest a slight shift of the recording electrode between bouts of ADS. A reliable switchable headstage that can automatically switch between recording and stimulation would allow for the microelectrodes to remain in their original sites. An advancement in electrode design and technology would eliminate these limitations.

It is possible that different ICMS parameters during the test bouts may be more effective for assessing EMG activity and evoked hindlimb movement after ADS therapy. Trains consisting of 13 stimulation pulses are most commonly used for evoking movement during motor cortex mapping procedures (Frost et al., 2013; Frost et al., 2015) and only 3 stimulation pulses were used during ICMS test bouts in this study. As a result, the shorter ICMS pulse train may not have allowed adequate temporal summation to activate the motor neurons (i.e., reach motor movement threshold) in the hindlimb spinal cord. Additionally, a more chronic application of ADS may be needed for the plasticity to result in functional motor recovery.

Finally, the present results were based on the topographic location of the electrodes through the dorsoventral depths of the spinal cord grey matter. The extracellular spike recordings were derived from a heterogeneous group of spinal cord neurons that were not specifically characterized. Likewise, the evoked spikes were the result of several polysynaptic pathways from hindlimb motor cortex, including ventral corticospinal, rubrospinal, reticulospinal and vestibulospinal tracts. The contribution of each of these spared pathways on the ability to drive post-SCI plasticity with ADS will need to be addressed, potentially using selective tract lesions in a similar neurophysiological preparation.

Conclusion

The significant increase in cortically-evoked firing of spinal cord neurons after acute ADS indicates a strengthening of the remaining descending pathways. ADS resulted in greater responsiveness in neurons throughout the dorsoventral depths of the spinal cord, and under a wide range of timing parameters. These results after an acute administration of ADS are promising for future neurorehabilitation and neuromodulatory interventions after moderate spinal cord injuries. A more chronic administration of ADS may elucidate the potential for ADS-mediated enhanced recovery of motor function after SCI.

Acknowledgments

This work was supported by the Paralyzed Veterans of America Research Foundation #3068, The Ronald D. Deffenbaugh Family Foundation, NIH/NINDS R01 NS030853, T32 Neurological and Rehabilitation Sciences Training Program, and NIH/NINDS F31 NS105442.

References

Akintunde A, Buxton DF (1992) Differential sites of origin and collateralization of corticospinal neurons in the rat: a multiple fluorescent retrograde tracer study. Brain Res 575:86-92.

Averna A, Pasquale V, Murphy MD, Rogantin MP, Van Acker GM, Nudo RJ, Chiappalone M, Guggenmos DJ (2019) Differential Effects of Open- and Closed-Loop Intracortical Microstimulation on Firing Patterns of Neurons in Distant Cortical Areas. Cereb Cortex.

Ballermann M, Fouad K (2006) Spontaneous locomotor recovery in spinal cord injured rats is accompanied by anatomical plasticity of reticulospinal fibers. Eur J Neurosci 23:1988-1996.

Basso DM, Beattie MS, Bresnahan JC (1995) A sensitive and reliable locomotor rating scale for open field testing in rats. J Neurotrauma 12:1-21.

Behrmann DL, Bresnahan JC, Beattie MS, Shah BR (1992) Spinal Cord Injury Produced by Consistent Mechanical Displacement of the Cord in Rats: Behavioral and Histological Analysis. J Neurotraum 9.

Bi G, Poo M (1998) Synaptic Modifications in Culutured Hippocampal Neurons: Dependence on Spike Timing, Synaptic Strength, and Postsynaptic Cell Type. The Journal of Neuroscience 18:10464-10472.

Bi G, Poo M (1999) Distributed synaptic modification in neural networks induced by patterned stimulation. Nature 401:792-796.

Bi G, Poo M (2001) Synaptic modification by correlated activity: Hebb's postulate revisited. Annu Rev Neurosci 24:139-166.

Borrell JA, Frost SB, Peterson J, Nudo RJ (2017) A 3D map of the hindlimb motor representation in the lumbar spinal cord in Sprague Dawley rats. Journal of neural engineering 14:016007.

Borrell JA, Krizsan-Agbas D, Nudo RJ, Frost SB (2020) Effects of a Contusive Spinal Cord Injury on Spinal Motor Neuron Activity and Conduction Time in Rats. Journal of Neural Engineering (Under Review).

Brown LT (1974) Rubrospinal projections in the rat. J Comp Neurol 154:169-187.

Capogrosso M et al. (2016) A brain-spine interface alleviating gait deficits after spinal cord injury in primates. Nature 539:284-288.

Casale EJ, Light AR, Rustioni A (1988) Direct projection of the corticospinal tract to the superficial laminae of the spinal cord in the rat. J Comp Neurol 278:275-286.

Debanne D, Gahwiler BH, Thompson SM (1994) Asynchronous pre- and postsynaptic activity induces associative long-term depression in area CA1 of the rat hippocampus in vitro. Proc Natl Acad Sci U S A 91:1148-1152.

Debanne D, Gahwiler BH, Thompson SM (1997) Bidirectional associative plasticity of unitary CA3-CA1 EPSPs in the rat hippocampus in vitro. Journal of neurophysiology 77:2851-2855.

Feldman DE (2012) The spike-timing dependence of plasticity. Neuron 75:556-571.

Frigon A (2017) The neural control of interlimb coordination during mammalian locomotion. Journal of neurophysiology 117:2224-2241.

Frost SB, Iliakova M, Dunham C, Barbay S, Arnold P, Nudo RJ (2013) Reliability in the location of hindlimb motor representations in Fischer-344 rats: laboratory investigation. Journal of neurosurgery Spine 19:248-255.

Frost SB, Dunham CL, Barbay S, Krizsan-Agbas D, Winter MK, Guggenmos DJ, Nudo RJ (2015) Output Properties of the Cortical Hindlimb Motor Area in Spinal Cord-Injured Rats. J Neurotrauma 32:1666-1673.

Fung TK, Law CS, Leung LS (2016) Associative spike timing-dependent potentiation of the basal dendritic excitatory synapses in the hippocampus in vivo. Journal of neurophysiology 115:3264-3274.

Gerstner W, Kempter R, van Hemmen JL, Wagner H (1996) A neuronal learning rule for sub-millisecond temporal coding. Nature 383:76-81.

Gilerovich EG, Moshonkina TR, Fedorova EA, Shishoko TT, Pavlova NV, Geraasimenko YP, Otellin VA (2008) Morphofunctional Characteristics of the Lumbar Enlargement of the Spinal Cords in Rats. Neuroscience and Behavioral Physiology 38:855-860.

Guggenmos DJ, Azin M, Barbay S, Mahnken JD, Dunham C, Mohseni P, Nudo RJ (2013) Restoration of function after brain damage using a neural prosthesis. PNAS 110:21177-21182.

Hebb DO (1949) The Organization of Behavior. Wiley, New York.

Hudson HM, Griffin DM, Belhaj-Saif A, Cheney PD (2015) Properties of primary motor cortex output to hindlimb muscles in the macaque monkey. Journal of neurophysiology 113:937-949.

Jackson A, Mavoori J, Fetz EE (2006) Long-term motor cortex plasticity induced by an electronic neural implant. Nature 444:56-60.

Krizsan-Agbas D, Winter MK, Eggimann LS, Meriwether J, Berman NE, Smith PG, McCarson KE (2014) Gait Analysis at Multiple Speeds Reveals Differential Functional and Structural Outcomes in Response to Graded Spinal Cord Injury. J Neurotraum 31:846-856.

Lemon RN (2008) Descending pathways in motor control. Annu Rev Neurosci 31:195-218.

Levy WB, Steward O (1983) Temporal contiguity requirements for long-term associative potentiation/depression in the hippocampus. Neuroscience 8:791-797.

Lewicki MS (1998) A review of methods for spike sorting: the detection and classification of neural action potentials. Network 9:R53-78.

Lisman J (1989) A mechanism for the Hebb and the anti-Hebb processes underlying learning and memory. Proc Natl Acad Sci U S A 86:9574-9578.

Markram H, Lubke J, Frotscher M, Sakmann B (1997) Regulation of Synaptic Efficacy by Coinicidence of Postsynaptic APs and EPSPs. Science 275:213-215.

Matsuyama K, Mori F, Kuze B, Mori S (1999) Morphology of Single Pontine Reticulospinal Axons in the Lumbar enlargement of the Cat: A Stud Using the Anterograde Tracer PHA-L. The Journal of Comparative Neurology 410:413-430.

McPherson JG, Miller RR, Perlmutter SI (2015) Targeted, activity-dependent spinal stimulation produces long-lasting motor recovery in chronic cervical spinal cord injury. Proc Natl Acad Sci U S A 112:12193-12198.

Mitchell EJ, McCallum S, Dewar D, Maxwell DJ (2016) Corticospinal and Reticulospinal Contacts on Cervical Commissural and Long Descending Propriospinal Neurons in the Adult Rat Spinal Cord; Evidence for Powerful Reticulospinal Connections. PLoS One 11:e0152094.

Molander C, Xu Q, Grant G (1984) The cytoarchitectonic organization of the spinal cord in the rat. I. The lower thoracic and lumbosacral cord. J Comp Neurol 230:133-141.

Moritz CT, Lucas TH, Perlmutter SI, Fetz EE (2007) Forelimb movements and muscle responses evoked by microstimulation of cervical spinal cord in sedated monkeys. Journal of neurophysiology 97:110-120.

Nishimura Y, Perlmutter SI, Eaton RW, Fetz EE (2013) Spike-timing-dependent plasticity in primate corticospinal connections induced during free behavior. Neuron 80:1301-1309.

Scheff SW, Rabchevsky AG, Fugaccia I, Main JA, Lumpp JE, Jr. (2003) Experimental modeling of spinal cord injury: characterization of a force-defined injury device. J Neurotrauma 20:179-193.

Schucht P, Raineteau O, Schwab ME, Fouad K (2002) Anatomical Correlates of Locomotor Recovery Following Dorsal and Ventral Lesions of the Rat Spinal Cord. Experimental neurology 176:143-153.

Skinner RD, Adams RJ, Remmel RS (1980) Responses of long descending propriospinal neurons to natural and electrical types of stimuli in cat. Brain Res 196:387-403.

Skinner RD, Coulter JD, Adams RJ, Remmel RS (1979) Cells of origin of long descending propriospinal fibers connecting the spinal enlargements in cat and monkey determined by horseradish peroxidase and electrophysiological techniques. J Comp Neurol 188:443-454.

Stent GS (1973) A physiological mechanism for Hebb's postulate of learning. Proc Natl Acad Sci U S A 70:997-1001.

Yang HW, Lemon RN (2003) An electron microscopic examination of the corticospinal projection to the cervical spinal cord in the rat: lack of evidence for cortico-motoneuronal synapses. Exp Brain Res 149:458-469.

Zimmermann JB, Jackson A (2014) Closed-loop control of spinal cord stimulation to restore hand function after paralysis. Frontiers in neuroscience 8:87.